

Phase Field Modeling of the $\text{Zn}_{1-x}\text{Cd}_x\text{O}$ Solid Solutions

I. SHTEPLIUK^{a,b,*}, N. PODOLSKAIA^{c,d,e} AND G. LASHKAREV^a

^aFrantsevich Institute for Problems of Materials Science, NASU, 03680, Kiev, Ukraine

^bDepartment of Physics, Chemistry and Biology, Linköping University, SE-58183 Linköping, Sweden

^cIoffe Physico-Technical Institute, RAS, Saint-Petersburg, Russia

^dSaint-Petersburg Branch of Joint Supercomputer Center, RAS, Saint-Petersburg, Russia

^eSt. Petersburg Academic University, Khlopinina 8/3, 194021 St. Petersburg, Russia

The analysis of spinodal decomposition in the $\text{Zn}_{1-x}\text{Cd}_x\text{O}$ ternary alloy was carried out by means of the nonlinear Cahn–Hilliard equation. Interaction parameter as a function of composition x was provided by valence force field simulations and was used in this analysis. The morphological patterns for the ternary alloys with different Cd content ($x = 5, 10, 50\%$) were experimentally obtained using the semi-implicit Fourier-spectral method. The simulated microstructure evolution $\text{Zn}_{0.95}\text{Cd}_{0.05}\text{O}$ demonstrates that the microstructure having a form of bicontinuous worm-like network is evolved with the progress of aging. An effect of the phase-field mobility and the gradient energy on the microstructure evolution of the $\text{Zn}_{1-x}\text{Cd}_x\text{O}$ alloys is discussed. It was found that the higher driving force for the decomposition in the higher Cd content film results in a higher decomposition rate revealed by the simulations. The temporal evolution of the simulated $\text{Zn}_{0.95}\text{Cd}_{0.05}\text{O}$ microstructure is in good agreement with experimental results, which have been obtained for this solid solution.

DOI: [10.12693/APhysPolA.126.1079](https://doi.org/10.12693/APhysPolA.126.1079)

PACS: 64.60.My, 05.70.Ln, 61.72.Bb, 61.72.Mm

1. Introduction

The $\text{Zn}_{1-x}\text{Cd}_x\text{O}$ ternary alloy has been subject to sizeable studies due to its importance as an active media in optoelectronic devices [1–9]. Previous investigations showed surprisingly that the $\text{Zn}_{1-x}\text{Cd}_x\text{O}$ thin films demonstrate chemical fluctuations causing an appearance of nanoscale cadmium-rich clusters [10]. This may be induced by a wide miscibility gap of the $\text{Zn}_{1-x}\text{Cd}_x\text{O}$ alloys [11]. On certain conditions the above-mentioned ternary alloys can be metastable or unstable and characterized by a phase separation on an atomic scale [12]. There is often a drastic permutation in materials properties if the phase separation proceeds. Singh et al. [13] reported that the high Cd content ($x \geq 0.15$) in the $\text{Zn}_{1-x}\text{Cd}_x\text{O}$ films grown by sol–gel method leads to films with mixed phases of Cd rich ZnO and cubic CdO along with Cd poor wurtzite ZnO. This phase segregation effects, by-turn, on a luminescence and phonon spectra of the deposited films [6, 13]. Other authors observed additional emission bands causing by the presence of the Cd-rich phases and the compositional fluctuations [10, 13, 14]. It was found that the alloy fluctuations in $\text{Zn}_{1-x}\text{Cd}_x\text{O}$ effect on the electrical properties of the $\text{Zn}_{0.94}\text{Cd}_{0.06}\text{O}/p\text{-SiC}$ heterostructures [8] and leads to a formation of the radiative recombination channels involving strongly localized excitons [9]. A direct evidence for the phase separation in the $\text{Zn}_{1-x}\text{Cd}_x\text{O}$ layers with $0.03 < x < 0.2$ has been obtained from the low temperature cathodoluminescence microscopy [10]. The phe-

nomenon of the phase separation in the $\text{Zn}_{1-x}\text{Cd}_x\text{O}$ was also investigated by means of a combination of the structural and the optical measurements [12]. It was found the appearance of the zinc-blende $\text{Zn}_{1-x}\text{Cd}_x\text{O}$ phase in addition to commonly discussed wurtzite and the rock-salt phases [12].

It should be mentioned that the phase separation of the unsteady states in semiconductor ternary alloys may be realized by the way of the spinodal decomposition [11]. The spinodal decomposition gives rise to the formation of the nanodomains (or macroscopic phases) of different composition, lowering the internal energy of the alloy [11]. Theoretical studies of the thermodynamic properties of the $\text{Zn}_{1-x}\text{Cd}_x\text{O}$ ternary alloy revealed that the spinodal decomposition occurs in the interval of $0.229 \leq x \leq 0.768$ for growth temperature of 793 K, and in the interval of $0.286 \leq x \leq 0.711$ for growth temperature of 923 K [11].

For all that the driving force provoking these fluctuations in $\text{Zn}_{1-x}\text{Cd}_x\text{O}$ solid solution has hitherto to be established. Studies of $\text{Zn}_{1-x}\text{Cd}_x\text{O}$ layers promise to provide a more complete comprehension of effects governing this phase separation, which is momentous to depositing layers of better homogeneity.

In this paper, the phase-field approach using the Cahn–Hilliard-type diffusion equation to generate a two-dimensional morphological evolution during the spinodal decomposition was utilized. The presented approach gives a possibility to find the numerical solution of pattern evolution of transforming phases.

2. Theoretical approach

In order to find out how the microstructure of the $\text{Zn}_{1-x}\text{Cd}_x\text{O}$ films depends on the Cd content in terms

*corresponding author; e-mail: shteplyuk_1987@ukr.net

of the spinodal decomposition, the non-linear Cahn–Hilliard diffusion equation can be applied [15]:

$$\frac{\partial x}{\partial t} = \nabla \cdot \left[M \nabla \left(\frac{\partial F}{\partial x} \right) \right], \quad (1)$$

where x is the composition of the cadmium (mole fraction), F is the total free energy of a system, M is the phase field mobility. $\frac{\partial F}{\partial x}$ denotes the first derivative in regard to composition. It should be mentioned that the functional form of the total free energy F in case of $\text{Zn}_{1-x}\text{Cd}_x\text{O}$ solid solution may be described by means of the following expression [16]:

$$F = \int_V \left[f(x) + U_i(x) + \frac{\kappa}{2} (\nabla x)^2 \right] dV, \quad (2)$$

where κ is a gradient energy coefficient, $f(x)$ is a Gibbs free energy, $U_i(x)$ is a strain energy. In this simulation, the contribution of the strain energy involving the film–substrate interaction to the total free energy was neglected.

Considering Eq. (2), and taking into account the fact that M is a constant for defined Cd content of the $\text{Zn}_{1-x}\text{Cd}_x\text{O}$ film, the temporal evolution of the compositional fields x is governed by the Cahn–Hilliard equation

$$\frac{\partial x}{\partial t} = \nabla \cdot \left[M \nabla \left(\frac{\partial f}{\partial x} + \frac{\partial U_i}{\partial x} - \kappa \nabla^2 x \right) \right], \quad (3)$$

where $f(x)$ and its first derivative may be determined as a function of Cd content

$$f(x) = \Omega x(1-x) + RT[x \ln x + (1-x) \ln(1-x)], \quad (4)$$

$$\frac{df}{dx} = \Omega(1-2x) + RT[\ln x - \ln(1-x)], \quad (5)$$

where Ω is an interaction parameter.

The chemical mobility M can be expressed as follows [17]:

$$M = (D/RT)x(1-x), \quad (6)$$

where M is a pre-factor which is equal to D/RT , D is a coefficient of interdiffusion, R is the gas constant, and T is a temperature. D can be expressed for $\text{Zn}_{1-x}\text{Cd}_x\text{O}$ pseudo-binary alloy system as follows:

$$D = D_{\text{Cd}}(1-x) + D_{\text{Zn}}x, \quad (7)$$

where D_{Cd} and D_{Zn} are diffusion coefficients of cadmium and zinc, correspondingly, and they can be described by an Arrhenius equation as follows [18]:

$$D = D_0 \exp\left(\frac{-\Delta E_a}{kT}\right), \quad (8)$$

where ΔE_a is an activation energy, D is a diffusivity.

The gradient energy coefficient κ can be expressed as follows [18]:

$$\kappa = \left(\frac{2}{3}\right) \Delta H_m r_0^2, \quad (9)$$

where ΔH_m is an enthalpy of the formation of the $\text{Zn}_{1-x}\text{Cd}_x\text{O}$ solid solution and r_0 is a nearest-neighbor distance. The enthalpy ΔH_m was determined according to the following conventional equation:

$$\Delta H_m = \Omega x(1-x). \quad (10)$$

Interaction parameter Ω as a function of composition x of $\text{Zn}_{1-x}\text{Cd}_x\text{O}$ ternary alloy was provided by valence force field (VFF) method [19, 20] using modified Keating’s potential (for non-ideal wurtzite) [21]. This parameter contains chemical contribution due to charge transfer and formation of bonds. The number of atoms in the each modelling crystal was 2048 and 20 computational runs were performed for the same solid composition, differing in the random group-II atomic distributions in the cation sublattice. The use of a large modelling crystal and many computational runs provided representative statistically independent atomic configurations in the modelling crystal and, consequently, is necessary for more accurate prediction of the interaction parameter [19]. It was found that Ω slightly decreases with increasing Cd content. This dependence can be approximated by means of the following analytical expression:

$$\Omega(x) = 15.657x + 16.904(1-x) + 0.659x(1-x). \quad (11)$$

Taking into account the non-linearity of the Cahn–Hilliard equation, its numerical solution can be obtained by means of the discretization in space and time. Equation (5) can be solved by the semi-implicit Fourier-spectral method [22, 23]. The discretized equation is expressed by

$$C^*(k, t + \Delta t) = \frac{C^*(k, t) - \Delta t M k^2 h^*(k, t)}{1 + 2\Delta t M k^4 \kappa}. \quad (12)$$

In Eq. (12) C^* and h^* represent the Fourier transform of composition field and h field, where h is equal to $\frac{\partial f}{\partial x} k = (k_1, k_2)$ is a vector in the Fourier space, $k = (k_1^2 + k_2^2)^{1/2}$ is the magnitude of k .

The following parameters were chosen for the simulation of the spinodal decomposition of the $\text{Zn}_{1-x}\text{Cd}_x\text{O}$ ternary alloy: $\Delta E_a = 2.26$ eV and $D = 0.6$ cm²/s (for Cd diffusion in ZnO [24]); $\Delta E_a = 2.66$ eV and $D = 1.57 \times 10^{-3}$ cm²/s (for Zn diffusion in ZnO [25]). The nearest-neighbor distance r_0 was taken from the literature [26]. This parameter was estimated as a distance between zinc and oxygen sites and found to be $R_{\text{Zn-O}} = 1.97$ Å in wurtzitic ZnO.

3. Results and discussions

It should be noted that the solution of the Cahn–Hilliard Eq. (5) was found in dimensionless form. The parameters were normalized by $\kappa^* = \frac{\kappa}{V E l^2}$, $M^* = \frac{M V}{L l^2}$, $\Delta x^* = \frac{\Delta x}{l}$ and $\Delta t^* = \frac{D \Delta t}{l^2}$, where E is a characteristic energy, which was chosen to be $E = 10^7$ J/m³, l is a characteristic length which is taken to be 2×10^{-9} m, V is atomic volume ($V = 13 \times 10^{-6}$ m³/mol) and L is a kinetic coefficient related to grain boundary mobility which is taken to be $L = 2.43 \times 10^{-10}$ Js/m³ [27]. The dimensionless grid size Δx^* was 1, and time step Δt^* for integration was chosen from the range of 0 to 1000000.

The $\text{Zn}_{1-x}\text{Cd}_x\text{O}$ alloy was approximated as a pseudo-binary system consisting of ZnO and CdO. The oxygen content is homogeneous throughout the simulation pattern. This model takes into consideration only sub-

stitution diffusion of the cadmium and the zinc in the metal (cation) sub-lattice of the hexagonal ZnO lattice. Here the noise value of 0.005 was used.

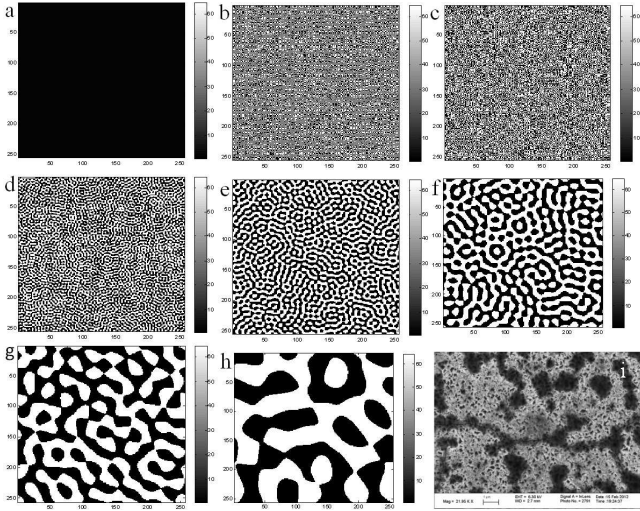


Fig. 1. Temporal evolution during phase separation of the $Zn_{0.95}Cd_{0.05}O$ solid solution: (a) $\Delta t^* = 0$, (b) $\Delta t^* = 1$, (c) $\Delta t^* = 10$, (d) $\Delta t^* = 100$, (e) $\Delta t^* = 1000$, (f) $\Delta t^* = 10000$, (g) $\Delta t^* = 100000$, (h) $\Delta t^* = 1000000$, (i) SEM image of $Zn_{0.95}Cd_{0.05}O$ film grown by dc magnetron sputtering onto sapphire substrates (the Cd-poor region is imaged bright and the Cd-rich region is dark).

An example of temporal evolution during phase decomposition obtained from Eq. (12) is demonstrated in Fig. 1. The system size is 256×256 in reduced units with periodic boundary conditions along both x and y directions. The real space grid size, $\Delta x^* = \Delta y^*$ is equal to 1.0. Figure 1 shows the two-dimensional simulation results for the phase decomposition of $Zn_{1-x}Cd_xO$ at 800 K. The average composition of the alloy is $Zn_{0.95}Cd_{0.05}O$. The local composition is represented by black scale, whereas the white region points a high concentration of cadmium. It is noteworthy that Fig. 1a is the initial state of the solid solution with a small composition fluctuation that is imposed as random noise. During early stages (Fig. 1b and c), it can be clearly seen that the initial fluctuations have grown in amplitude. An increase in aging time gives rise to enhance the alloy fluctuations. The Cd-rich phase with a droplet form is nucleated in places (see Fig. 1d-f). With progress of aging, as seen from Figs. 1g and h, microstructure coarsening occurs by the mechanism of the Ostwald ripening. In other words, the Cd-rich and Cd-poor regions form a bicontinuous worm-like network that undergoes coarsening when the $\Delta t^* \geq 100$. It is obvious that only after about $\Delta t^* = 10000$, the composition of the Cd-rich and Cd-poor regions reach the equilibrium values. It is interesting that the simulation results agree well with the experimental results, which are presented for comparison in Fig. 1i. Using the dc (direct current) magnetron sputtering we have grown the $Zn_{0.95}Cd_{0.05}O$ film onto sapphire substrate. A study of the scanning electron microscopy (SEM) revealed that

the film is composed by the Cd-rich (dark) and Cd-poor regions, as was evidenced by a selective elemental analysis using energy-dispersive X-ray spectroscopy. Evidently that the microstructure depicted in Fig. 1i is similar to the morphological pattern presented in Fig. 1h.

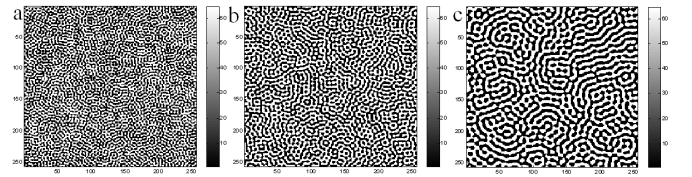


Fig. 2. Morphological patterns during the spinodal decomposition and the subsequent coarsening (with unchanged value of $\Delta t^* = 100$): (a) 5% Cd, (b) 10% Cd, (c) 50% Cd. The black color represents the Cd-poor region and the white is referred to the Cd-rich phase.

Figure 2 shows the microstructural evolution predicted for the $Zn_{1-x}Cd_xO$ alloys with the cadmium content of 5, 10 and 50% for the case of $\Delta t^* = 100$. The interconnected microstructure is more clearly observed in the case of the alloy with 50 at.% Cd than at that corresponding to the other alloy composition. This type of the morphology is proper to early stages of the spinodal decomposition [28]. This fact can be attributed to the higher driving force for the phase decomposition in the $Zn_{1-x}Cd_xO$ alloy with $x = 0.5$. Generally speaking, the driving force for the decomposition is the minimization of the systems Gibbs free energy.

In presented simulations, there are two contributions to the driving force in the Cahn–Hilliard equation, Eq. (3): the Cd content-dependent free energy of mixing and the Cd content-dependent gradient energy. The gradient energy coefficient can be related with the interaction energy between the phases. If this parameter increases, the increase in the interaction energies takes place. It means that more similar phase particles come close to each other than before. It can also be related with diffused boundary width. An enlargement of the gradient energy may lead to enhancement of the width of the diffused phase boundary. We have, nevertheless, revealed that the interaction parameter in $Zn_{1-x}Cd_xO$ solid solutions and gradient energy decrease with increase of the Cd content. On the other hand, the increase in the Cd content causes the enhancement of the phase mobility according to Eq. (6). Growth of the mobility induces the increases in particle speed. Taking into account the fact that the Cahn–Hilliard equation is a modified form of the Fick law for the transient diffusion equation it may be concluded that mobility can be linked with a speed of the microstructure evolution. Thereby, the magnitude of the mobility will make a difference in the time taken by the system to reach an equilibrium state, i.e., the larger mobility indicates the system has lesser time to move towards equilibrium. As it can be clearly seen from the above figures, the coarsening of the microstructure is the largest for 50 at.% Cd ($M = 0.08724$) than for other Cd contents.

4. Conclusions

In this paper, the semi-implicit Fourier spectral method was used for the solving the Cahn–Hilliard equation with the Cd content-dependent mobility and the gradient energy coefficient. The temporal evolution of the microstructure during spinodal decomposition in $\text{Zn}_{0.95}\text{Cd}_{0.05}\text{O}$ solid solution was simulated. The compositional dependence of the $\text{Zn}_{1-x}\text{Cd}_x\text{O}$ interaction was computed by valence force field method and was used to analyze spinodal decomposition. It was revealed that the small compositional fluctuation leads to a spontaneous phase separation, producing a two-dimensionally interconnected microstructure. The microstructure coarsening was observed at the increase of the aging time. The presented simulations show that the decomposition is initiated faster for higher Cd contents. The higher Cd content film has larger driving force for the decomposition due to the chemical mobility and the free energy of mixing, which give the largest contribution at $x = 0.5$ than at $x = 0.05$ and 0.1 . The temporal development of the simulated $\text{Zn}_{0.95}\text{Cd}_{0.05}\text{O}$ microstructure is in good agreement with experimental results, which have been obtained for this solid solution.

Acknowledgments

This publication is part of Dr. I. Shtepliuk research work at Linköping University, thanks to a Swedish Institute scholarship. Dr. N. Podolskaia gratefully acknowledges financial support of the Russian Science Foundation under the Grant No.14-22-00018.

References

- [1] J. Muth, A. Osinsky, in: *Wide Bandgap Light Emitting Materials and Devices*, Eds. G.F. Neumark, I.L. Kuskovsky, H. Jiang, Wiley-VCH Verlag, Weinheim 2007, p. 179.
- [2] S. Kalusniak, S. Sadofev, J. Puls, F. Henneberger, *Laser Photonics Rev.* **3**, 233 (2009).
- [3] I. Shtepliuk, *Superlatt. Microstruct.* **71**, 62 (2014).
- [4] I. Shtepliuk, G. Lashkarev, O. Khyzhun, B. Kowalski, A. Reszka, V. Khomyak, V. Lazorenko, I. Timofeeva, *Acta Phys. Pol. A* **120**, 914 (2011).
- [5] I. Shtepliuk, G. Lashkarev, V. Khomyak, P. Marianchuk, P. Koreniuk, D. Myroniuk, V. Lazorenko, I. Timofeeva, *Acta Phys. Pol. A* **120**, A61 (2011).
- [6] I. Shtepliuk, O. Khyzhun, G. Lashkarev, V. Khomyak, V. Lazorenko, *Acta Phys. Pol. A* **122**, 1034 (2012).
- [7] I. Shtepliuk, G. Lashkarev, V. Khomyak, O. Lytvyn, P. Marianchuk, I. Timofeeva, A. Ievtushenko, V. Lazorenko, *Thin Solid Films* **520**, 4772 (2012).
- [8] I. Shtepliuk, V. Khranovskyy, G. Lashkarev, V. Khomyak, V. Lazorenko, A. Ievtushenko, M. Syväjärvi, V. Jokubavicius, R. Yakimova, *Solid State Electron.* **81**, 72 (2013).
- [9] I. Shtepliuk, V. Khranovskyy, G. Lashkarev, V. Khomyak, A. Ievtushenko, V. Tkach, V. Lazorenko, I. Timofeeva, R. Yakimova, *Appl. Surf. Sci.* **276**, 550 (2013).
- [10] F. Bertram, S. Giemisch, D. Forster, J. Christen, R. Kling, *Appl. Phys. Lett.* **88**, 061915 (2006).
- [11] I.I. Shtepliuk, *Acta Phys. Pol. A* **124**, 865 (2013).
- [12] V. Venkatachalapathy, A. Galeckas, M. Trunk, T. Zhang, A. Azarov, A.Yu. Kuznetsov, *Phys. Rev. B* **83**, 125315 (2011).
- [13] A. Singh, D. Kumar, P.K. Khanna, M. Kumar, B. Prasad, *ECS J. Solid State Sci. Technol.* **2**, 136 (2013).
- [14] C.W. Sun, P. Xin, C.Y. Ma, Z.W. Liu, Q.Y. Zhang, Y.Q. Wang, Z.J. Yin, S. Huang, T. Chen, *Appl. Phys. Lett.* **89**, 181921 (2006).
- [15] J.W. Cahn, *Acta Metall.* **9**, 795 (1961).
- [16] L.-Q. Chen, *Annu. Rev. Mater. Res.* **32**, 113 (2001).
- [17] T.W. Heo, S. Bhattacharyay, L.-Q. Chen, *Philos. Mag.* **93**, 1468 (2013).
- [18] S.L. Alvarez, E.O. Avila-Davila, V.M. Lopez-Hirata, J.L. Gonzalez-Velazquez, *J. Mater. Res.* **16**, 975 (2013).
- [19] S.Yu. Karpov, N.I. Podolskaya, I.A. Zhmakin, A.I. Zhmakin, *Phys. Rev. B* **70**, 235203 (2004).
- [20] R.M. Martin, *Phys. Rev. B* **10**, 4005 (1970).
- [21] T. Takayama, M. Yuri, K. Itoh, T. Baba, J.S. Harris Jr., *J. Cryst. Growth* **222**, 29 (2001).
- [22] J. Zhu, L.-Q. Chen, J. Shen, V. Tikare, *Phys. Rev. E* **60**, 3564 (1999).
- [23] L.-Q. Chen, J. Shen, *Comput. Phys. Commun.* **108**, 147 (1998).
- [24] A.Yu. Azarov, T.C. Zhang, B.G. Svensson, A.Yu. Kuznetsov, *Appl. Phys. Lett.* **99**, 111903 (2011).
- [25] J. Serrano, A.H. Romero, F.J. Manjon, R. Lauck, M. Cardona, A. Rubio, *Phys. Rev. B* **69**, 094306 (2004).
- [26] C. Guglieri, E. Céspedes, C. Prieto, J. Chaboy, *J. Phys. Condens. Matter* **23**, 206006 (2011).
- [27] J. Deng, S. Rokkam, *Mater. Trans.* **52**, 2126 (2011).
- [28] J.E. Hilliard, in: *Spinodal Decomposition*, Ed. H.I. Aaronson, Metals Park, Ohio ASM 1970, p. 497.